Selective chemical recycling of polyhydroxybutyrate into high-value hydroxy acid using Taurine organocatalyst

Elena Gabirondo[1], Ainhoa Maiz-Iginitz[1,2], Marta Ximenis[1], Katarzyna Świderek[3], Daniel Andrés-Sanz[2], Vicent Moliner[3], Luis Cabedo[4], Andrea H. Westlie[5], Eugene Y.-X. Chen[5], Daniel Alonso Cerrón-Infantes[6,7,8], Miriam M. Unterlass[6,7,8], Fernando López-Gallego[2,9], Agustin Etxeberria[1] and Haritz Sardon[1,*]

[1] POLYMAT and Department of Polymers and Advanced Materials: Physics, Chemistry and Technology, Faculty of Chemistry, University of the Basque Country UPV/EHU, P° Manuel de Lardizabal, 3, 20018 Donostia-San Sebastian, Spain.

[2] Center for Cooperative Research in Biomaterials (CIC biomaGUNE), Basque Research and Technology Alliance (BRTA), Paseo de Miramon 182, San Sebastián, Spain.

[3] BioComp Group, Institute of Advanced Materials (INAM), Universitat Jaume I, 12071 Castellón, Spain.

[4] Polymers and Advanced Materials Group (PIMA), Universitat Jaume I (UJI), Avenida de Vicent Sos Baynat s/n, 12071 Castelló, Spain.

[5] Department of Chemistry, Colorado State University, Fort Collins, CO 80523-1872, USA.

[6] Fraunhofer Institute for Silicate Research ISC, Neunerplatz 2, 97082 Wuerzburg, Germany.

[7] Julius Maximilian University of Wuerzburg, Chair of Chemical Technologie of Materials Synthesis, Roentgenring 11, 97070 Wuerzburg, Germany.

[8] CeMM – The Research Center for Molecular Medicine of the Austrian Academy of Sciences, Lazarettgasse 14, AKH BT 25.3, 1090 Vienna, Austria.

[9] IKERBASQUE, Basque Foundation for Science, María Díaz de Haro 3, 48013 Bilbao, Spain.

Materials

Poly(*R*)-3-hydroxybutyric acid was obtained from Sigma Aldrich S.A. All the catalyst employed were from Sigma Aldrich S.A.: *p*-toluenesulfonic acid (pTSA) (95 %), methanesulfonic acid (MSA) (99 %), benzoic acid (BA) (99.5 %), hydrochloric acid (HCl) (37 %), sulfuric acid (H_2SO_4) (95 %), acetic acid (>99 %), creatine (99 %), taurine (>99 %) and sodium hydroxide (NaOH) (>98 %). PHBV polymer was purchased from Biomer Biopolyesters (Schwalbach/Germany) and PHBH from Kaneka Corporation (Osaka, Japan) and used as received. Diethyl ether was acquired from Fischer Scientific and was used without any further purification.

Methods

^{1}H and ^{13}C Nuclear Magnetic Resonance (NMR)

^{1}H and ^{13}C Nuclear Magnetic Resonance (NMR) spectroscopy was recorded in a Bruker Avance DPX 300 at 300.16 MHz and at 75.5 MHz of resonance frequency respectively, using deuterated chloroform ($CDCl_3$), deuterated dimethyl sulfoxide (DMSO) or deuterium oxide (D_2O) as solvent at room temperature. Experimental conditions were as follows: a) for ^{1}H NMR spectroscopy: 10 mg of sample; 3 s acquisition time; 1 s delay time; 8.5 µs pulse; spectral width 5000 Hz and 32 scans; b) for ^{13}C NMR spectroscopy: 40 mg; 3 s acquisition time; 4 s delay time; 5.5 µs pulse; spectral width 18800 Hz and more than 10000 scans.

Differential Scanning Calorimetry (DSC)

Differential scanning calorimetry (DSC) measurements were performed using a DSC8500 from Perkin Elmer, Inc. calibrated with indium and tin standards. The DSC scans were performed with approximately 5 mg of sample at a heating rate of 20 °C/min from -20 °C to 180 °C under a nitrogen flow rate of 20 mL/min.

Thermogravimetric analysis (TGA)

Thermogravimetric analysis (TGA) was carried out using a Q500 Thermogravimetric Analyzer from TA Instruments. Samples were heated from room temperature to 600 °C at a rate of 10 °C/min under a constant N_2 flow.

Matrix Assisted Laser Desorption Ionization - Time of Flight (MALDI-TOF) analysis

MALDI-TOF measurements were performed on a Bruker Autoflex Speed system (Bruker, Germany) instrument, equipped with a 355 nm NdYAG laser using chloroform as solvent and DCTB-NaTFA substrate.

GC-FID chromatogram

100 mM solutions were prepared from solid reaction products or commercial standards. The samples were derivatized with a similar protocol as the one described by Cheong et al.[1].Briefly, the reaction or standard samples (100 µL) were acidified with 6 M HCl and extracted with ethyl acetate 1:1. 50 µL of the extracted sample were incubated with 50 µL of a 1:1 (*v:v*) mixture of N-Methyl-N-tert-butyldimethylsilyltrifluoroacetamide (MTBSTFA) and ethyl acetate for 1h at 60 °C. The samples were dried with the addition of anhydrous $MgSO_4$ before GC analysis. Derivatized samples were analyzed by GC-FID as described by Orrego et al.[2] in an Agilent 8890 System using a Beta DEXTM 120 Capillary Column (30 m x 0.25 mm x 0.25 µm) and helium as carrier gas. The temperature of the injector and FID detector was 280 °C and 300°C respectively. The initial

temperature of the column (80 °C) was increased up to 150 °C at a rate of 2 °C min^{-1}, then it was maintained for 5 minutes before increasing the temperature up to 200 °C at a 20 °C min^{-1} rate, the temperature was maintained at 200 °C for 2 minutes. Retention times were 22.41 for the derivatized (*S*)-3-hydroxybutyric acid standard and 22.51 for the derivatized (*R*)-3-hydroxybutyric acid standard.

Depolymerization procedure of PHB

The depolymerization of PHB was carried out by hydrolysis in order to obtain hydroxy acid monomers. For that, in a high-pressure Schlenk tube 1g (0.012 mol) of PHB polymer, 15 equivalents (0.174 mol, 3.14 mL) of water, and 10 mol % (respect the repeating unit of the polymer) of catalyst, (in the case of taurine 0.001 mol, 0.145 g) were added. The vessel was submerged in a pre-heated oil bath at 180 °C until the disappearance of the polymer was observed. After the depolymerization reaction was finished, the Schlenk tube was removed from the bath and it was let cool down until room temperature. The reactions were monitored by ^{1}H NMR to track the conversion to HBA and the formation of CA side product. Aliquots were taken directly from the reaction medium without quenching, and deuterated water was added to perform the NMR analysis. If solid residue remained, the mixture was first filtered to separate and weigh the solid fraction before analyzing the liquid phase by ^{1}H NMR.

Purification procedure of HBA

After the depolymerization process, the reaction media was filtered to remove any residual polymer that was not depolymerized or any other solid particles. Afterward, ethanol was added and the catalyst, taurine, was precipitated and filtered. In order to separate both products (HBA and CA), liquid-liquid extraction with diethyl ether was carried out. The CA goes to the organic phase and the HBA monomer remains in the water phase. Once the CA was removed from the media, the HBA dissolved in water was dried to obtain pure HBA, confirmed by ^{1}H NMR and MALDI-TOF.

Table S1. Quantitative values of depolymerization of PHB into HBA and CA.

Catalyst	Depolymerization (%)	HBA (%)	CA (%)

pTSA	82	34	48
MSA	78	38	40
BA	90	69	21
AcOH	100	80	20
H_2SO_4	72	43	29
HCl	70	37	33
NaOH	70	30	40
Taurine	100	98	2
Creatine	72	39	33

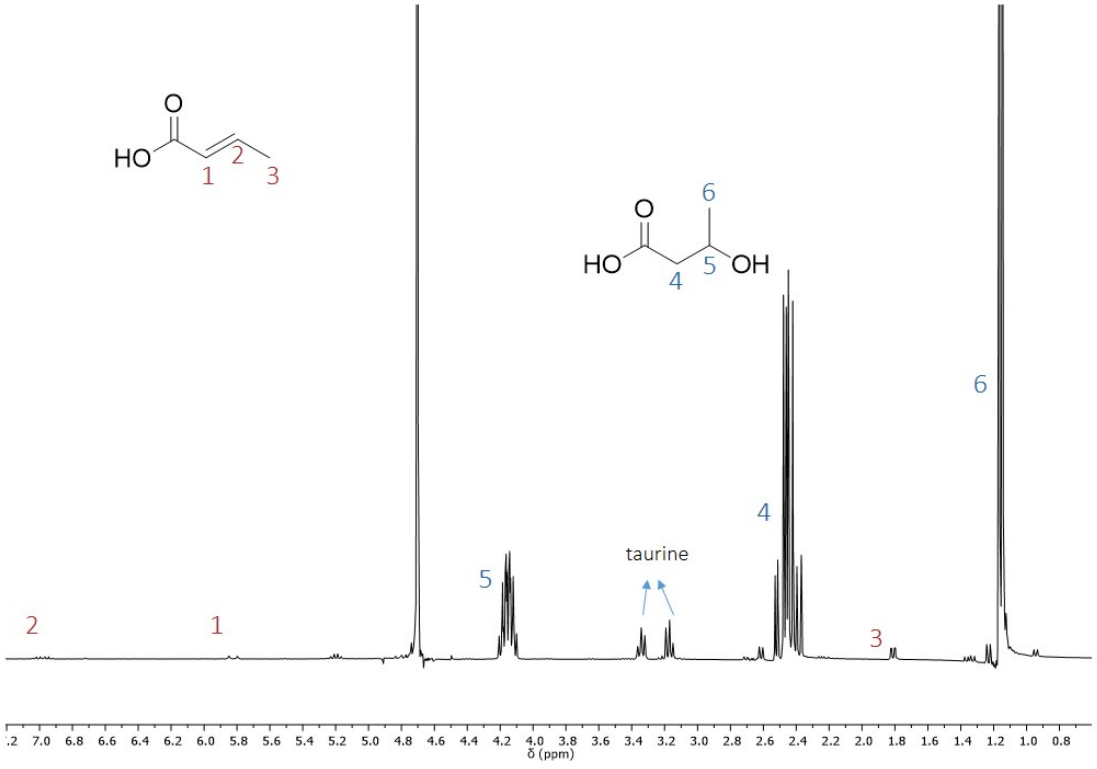

Figure S1. ^{1}H NMR of the depolymerization of PHB into HBA and CA.

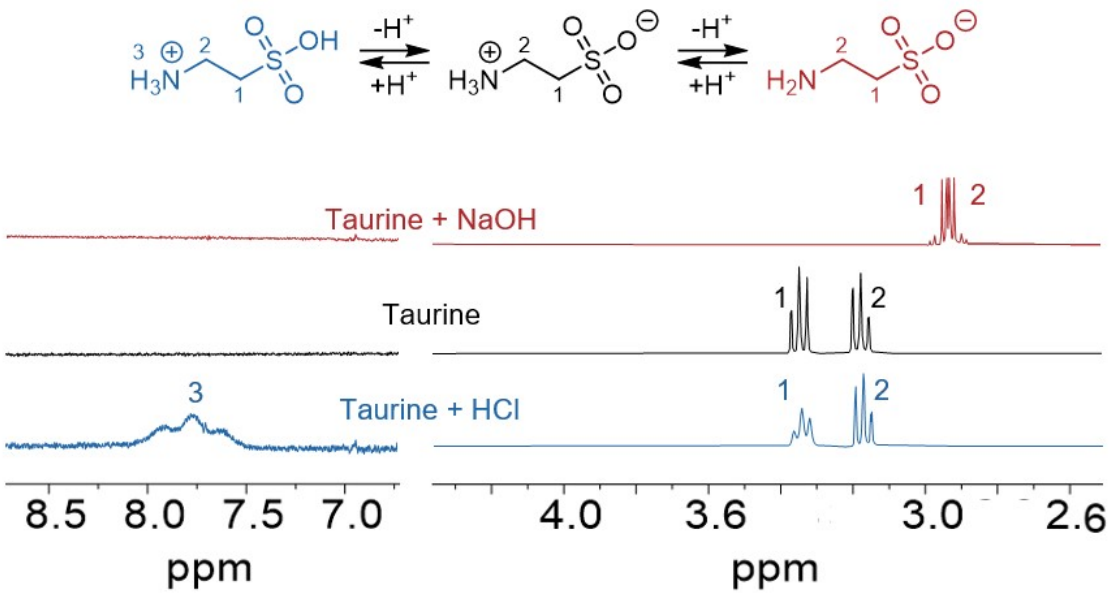

Figure S2. ^{1}H NMR of taurine in basic media pH 10 (red), neutral media (black) and acidic media pH 3(blue).

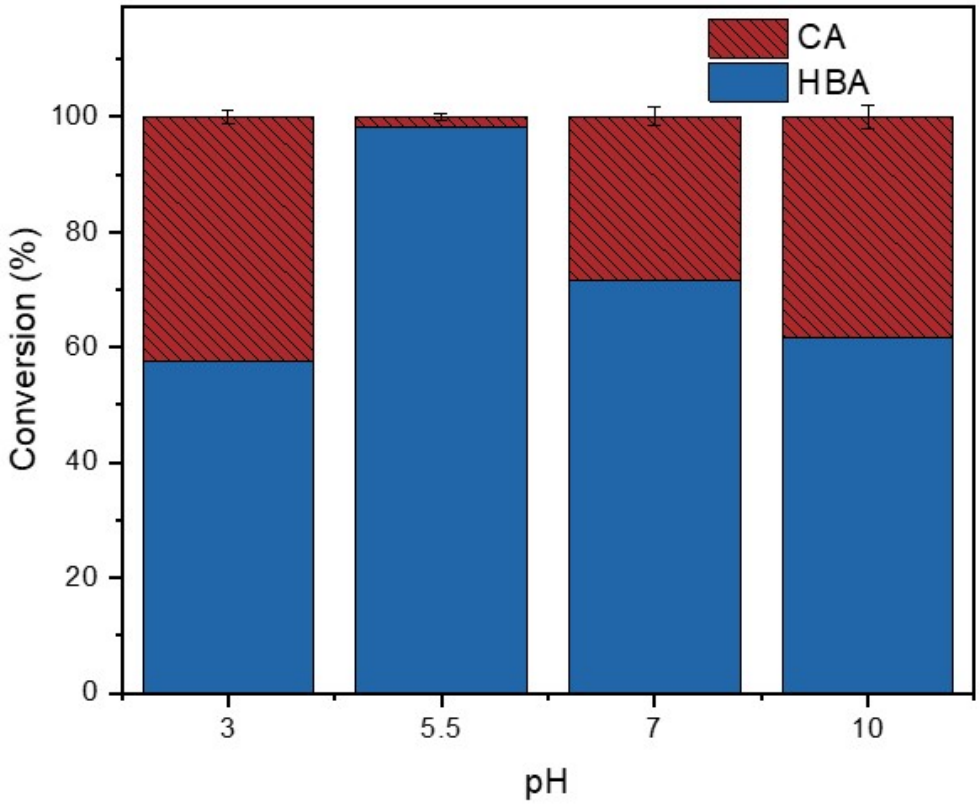

Figure S3. The effect of the pH in the depolymerization process.

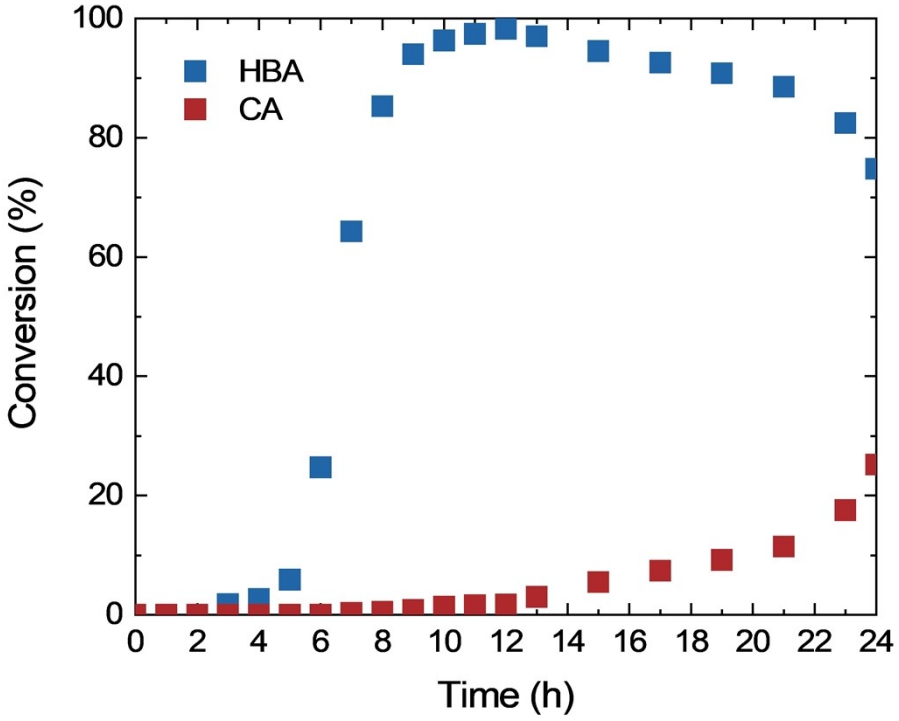

Figure S4. Kinetic of the conversion of HBA and CA from PHB depolymerization.

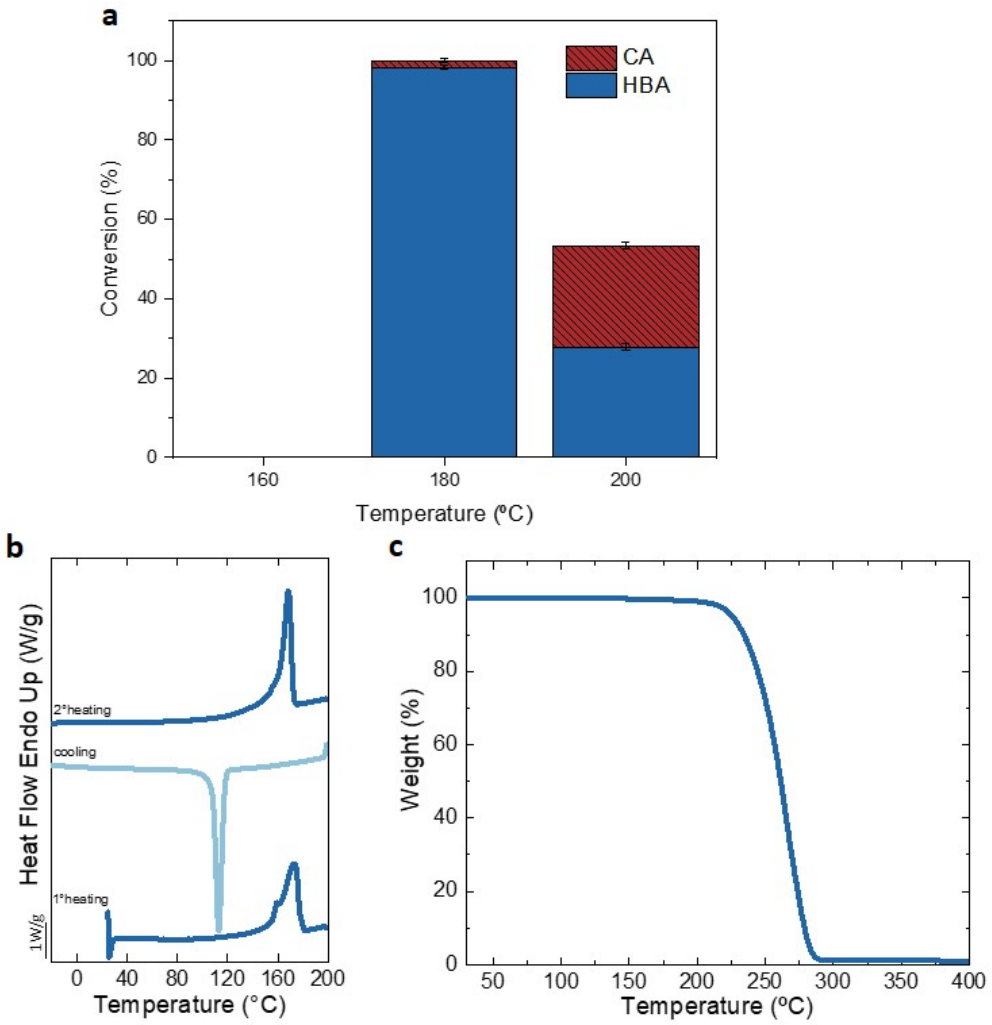

Figure S5. a) Effect of the temperature on the depolymerization of PHB, b) DSC results of PHB and c) TGA analysis of PHB under nitrogen flow.

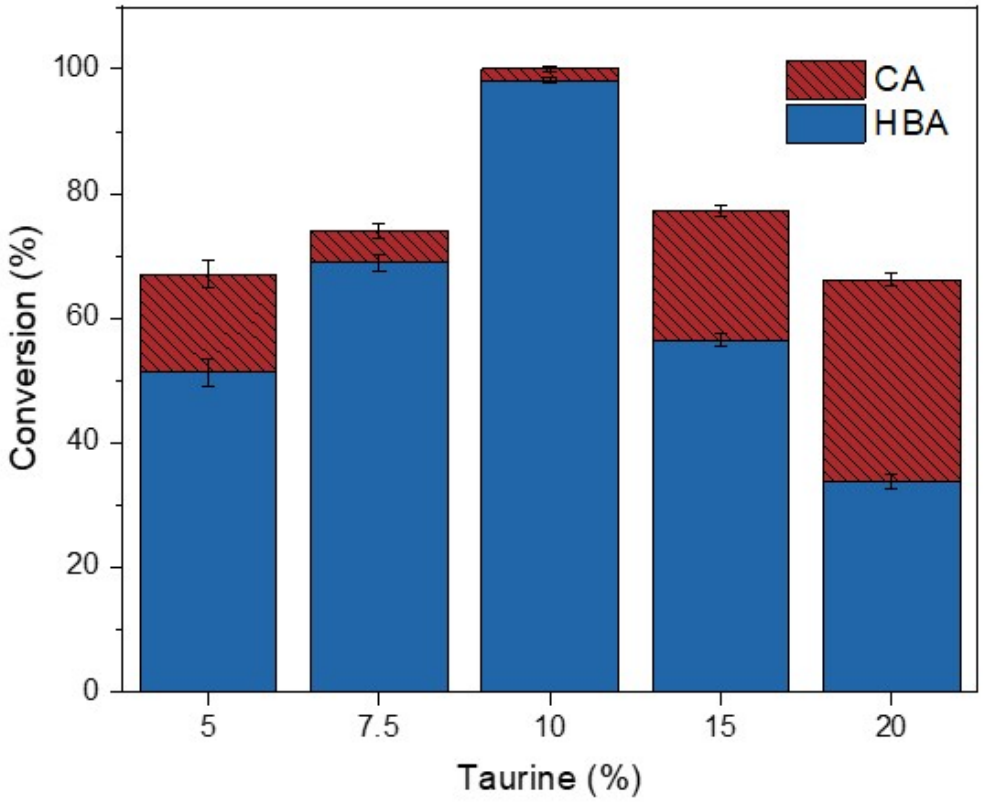

Figure S6. The effect of the taurine loading in the depolymerization process.

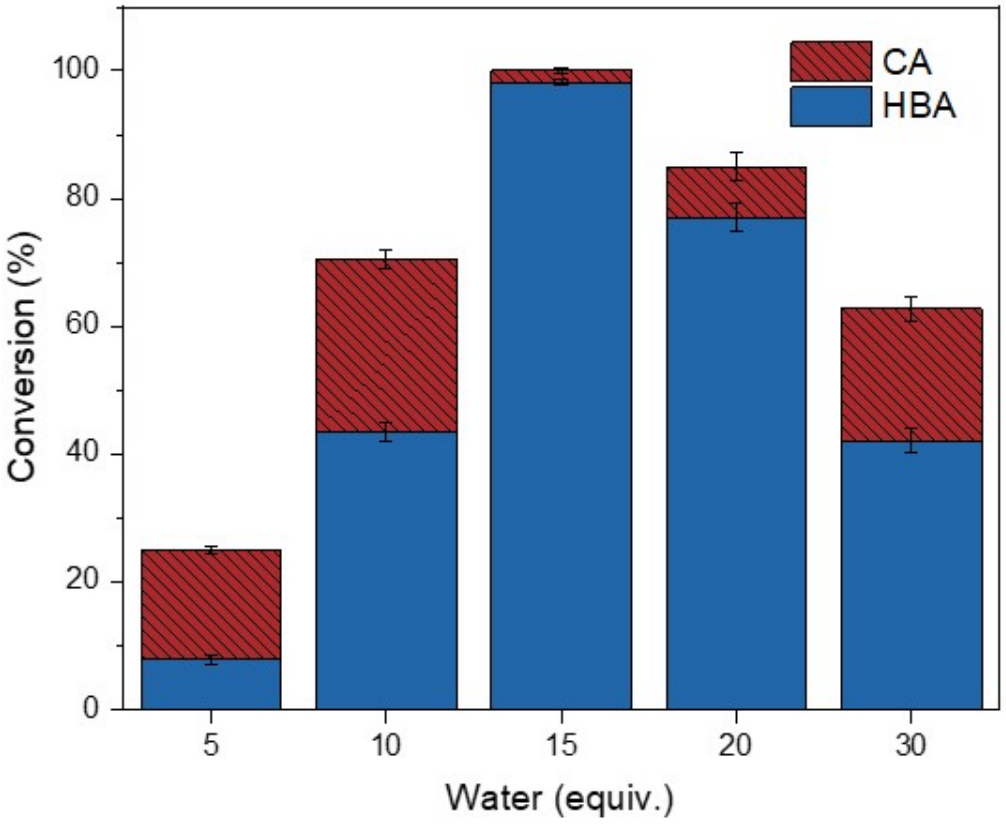

Figure S7. The effect of the water equivalents in the depolymerization process when using 10 % of taurine.

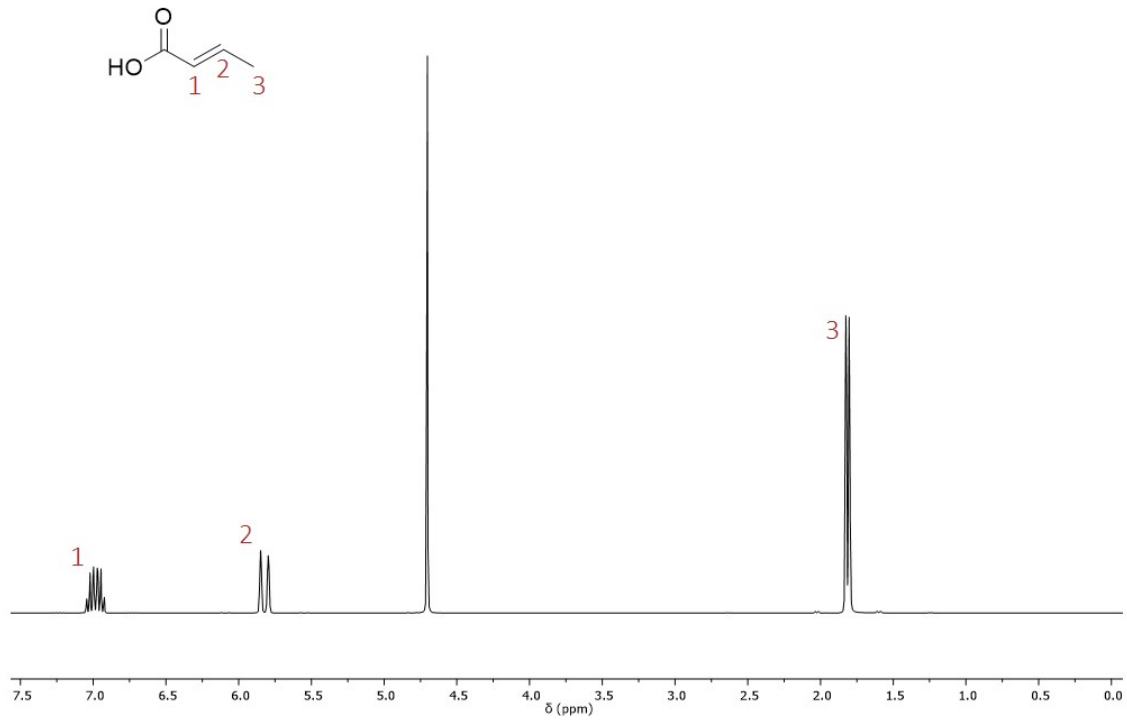

Figure S8. ^{1}H NMR spectrum of CA after the distillation process of the depolymerization mixture.

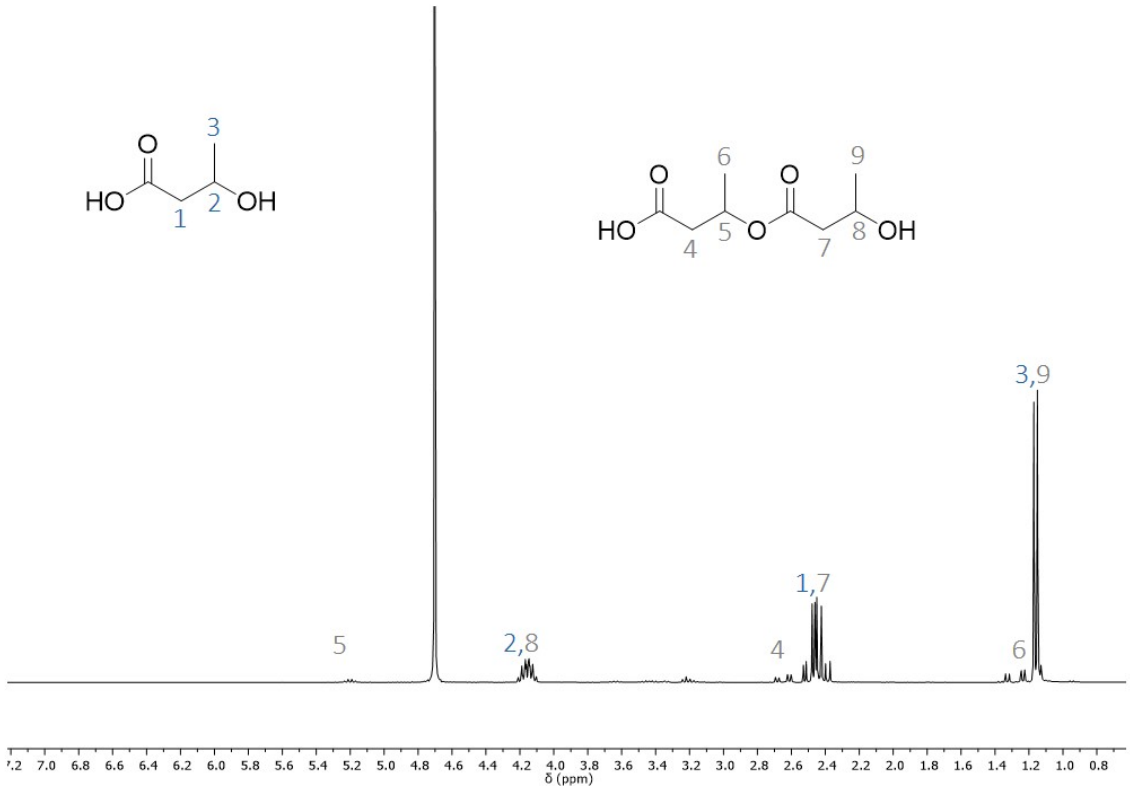

Figure S9. ^{1}H NMR spectrum of HBA monomer and traces of dimer after purification.

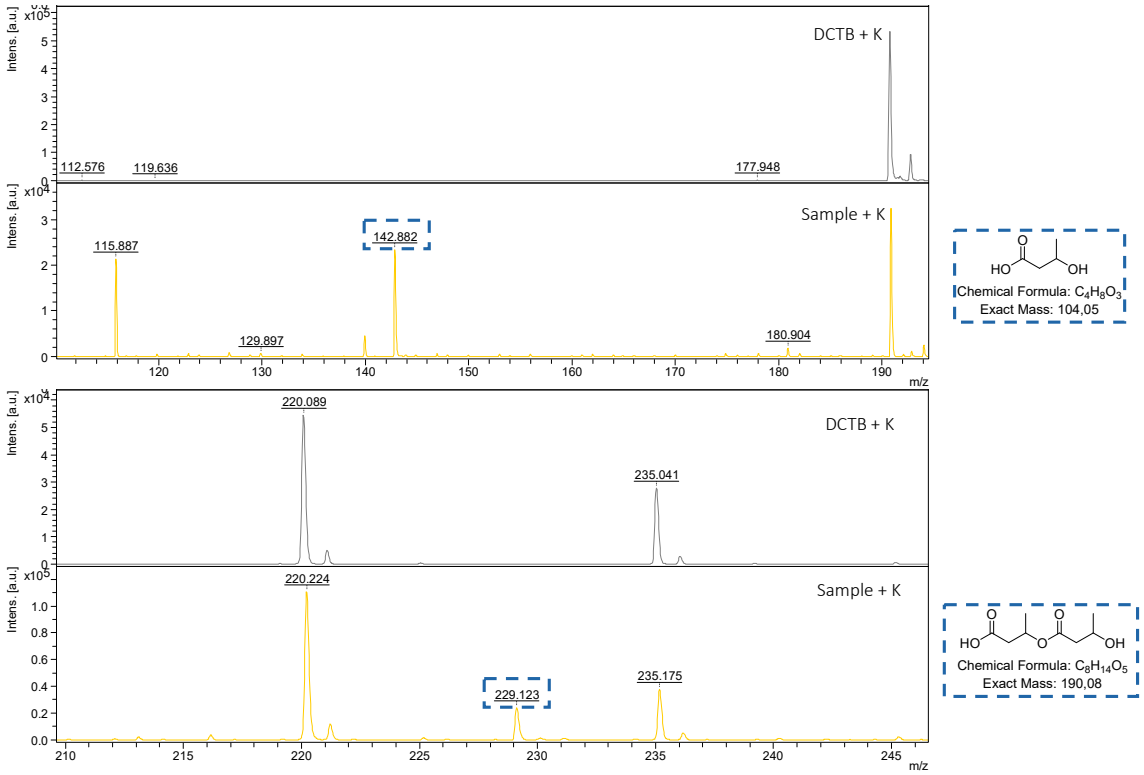

Figure S10. MALDI-TOF spectra of HBA monomer and dimer after purification.

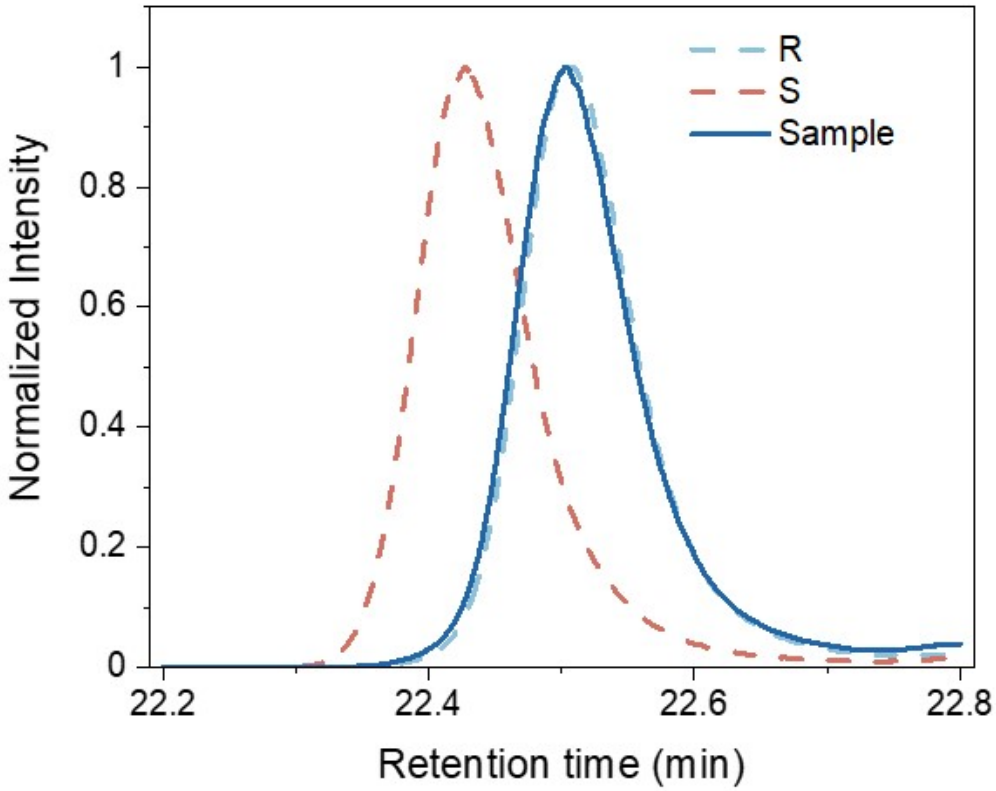

Figure S11. Normalized GC-FID chromatogram for the resolution of the enantiomers of the 3-hydroxybutyric acid standards and reaction sample. (R)-3-hydroxybutyric acid standard (blue dashed line), (S)-3-hydroxybutyric acid (red dashed line), and reaction product (blue line).

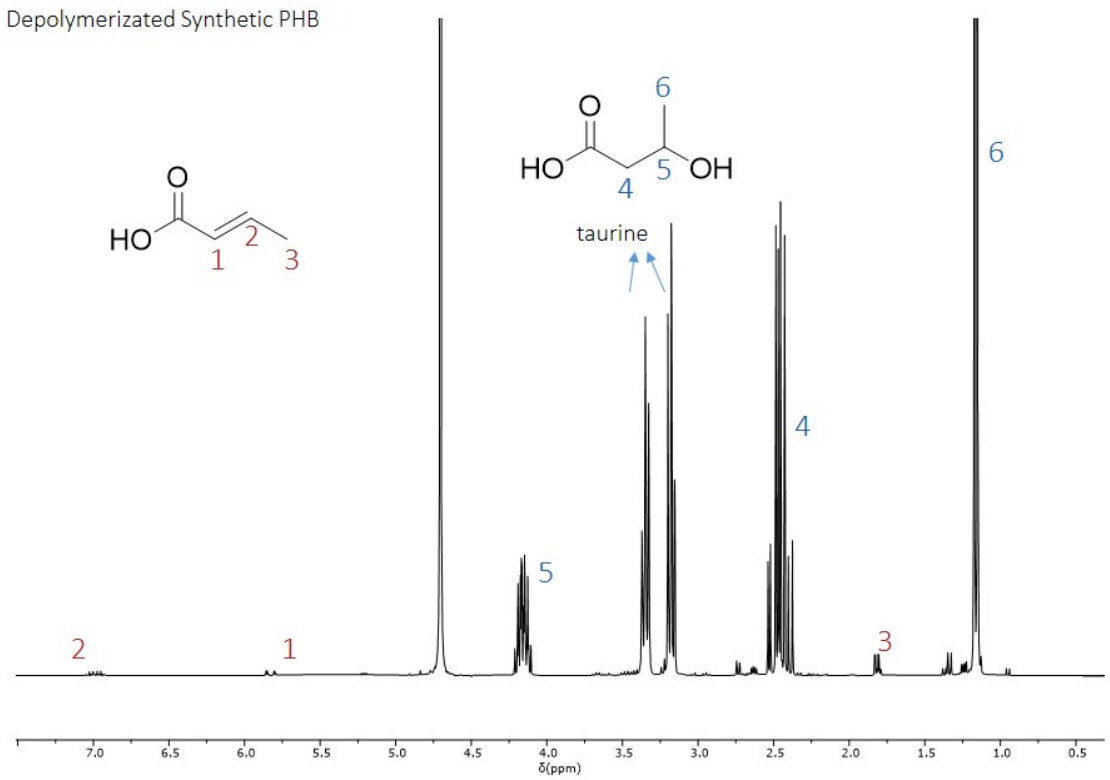

Figure S12. ^{1}H NMR of the depolymerization of synthetic PHB.

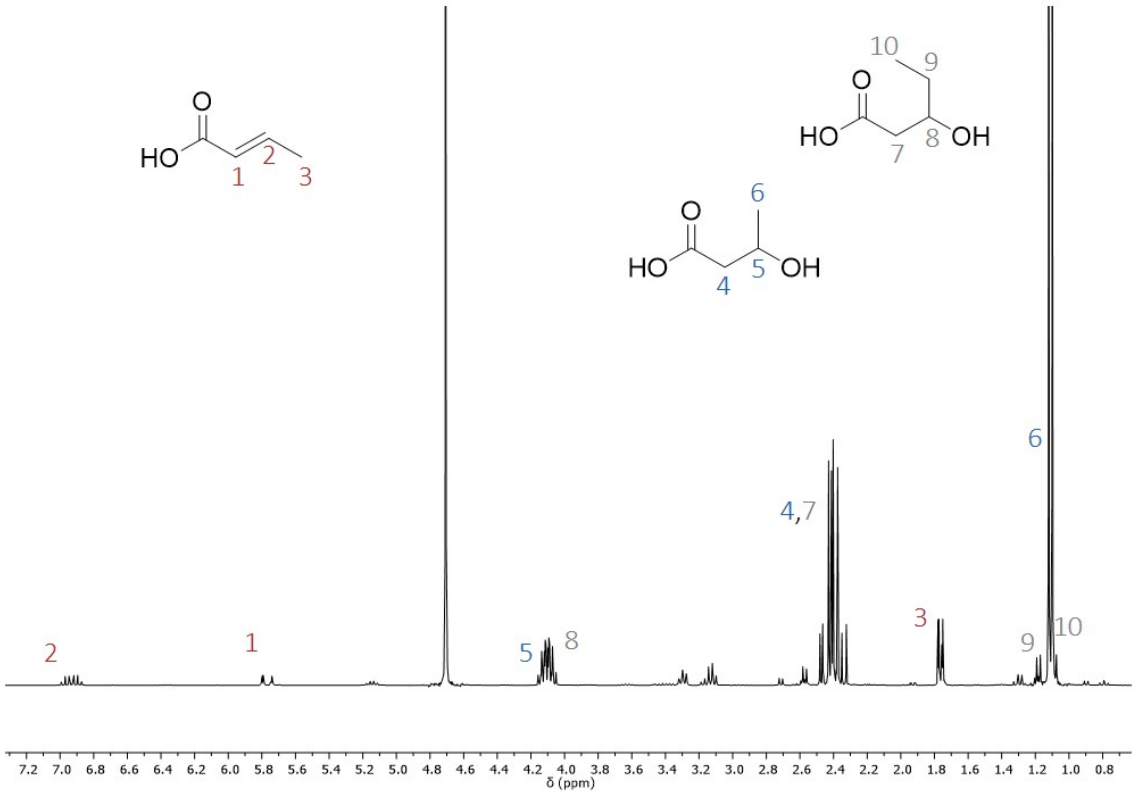

Figure S13. ^{1}H NMR of the depolymerization of PHBV into HBA, CA and HVA.

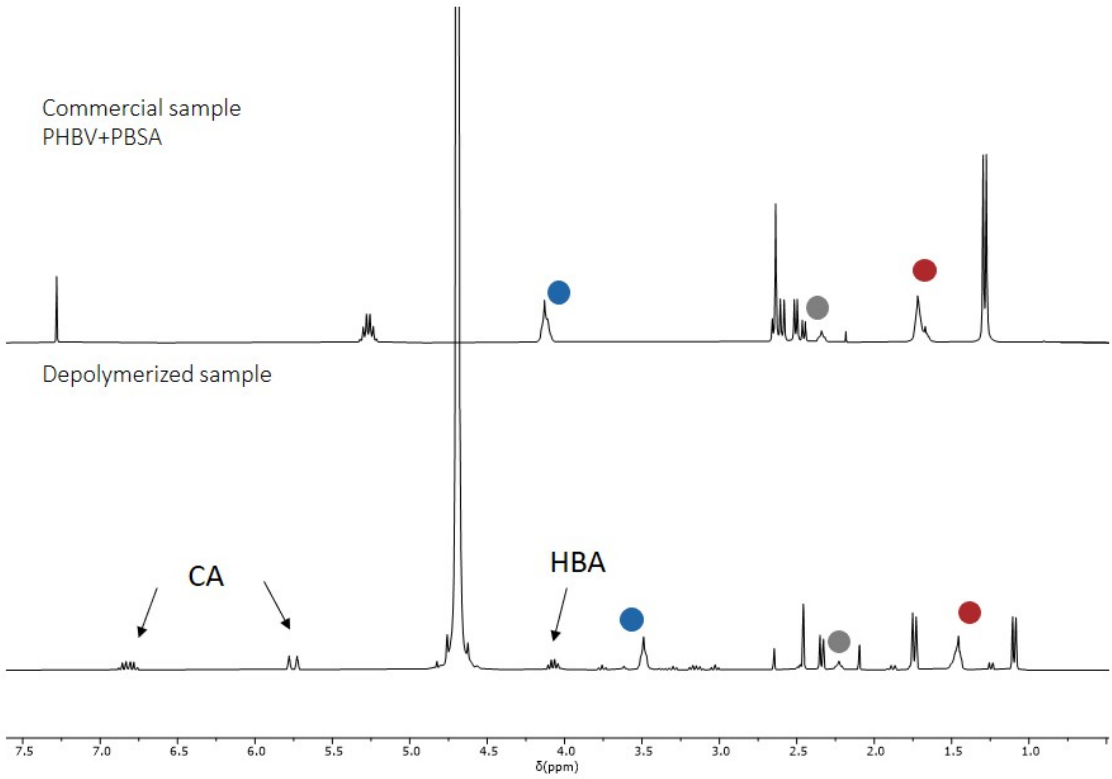

Figure S14. ^{1}H NMR comparison of commercial sample PHBV+PBSA with the depolymerized sample. The colored circles indicate the presence of PBSA before and after the depolymerization.

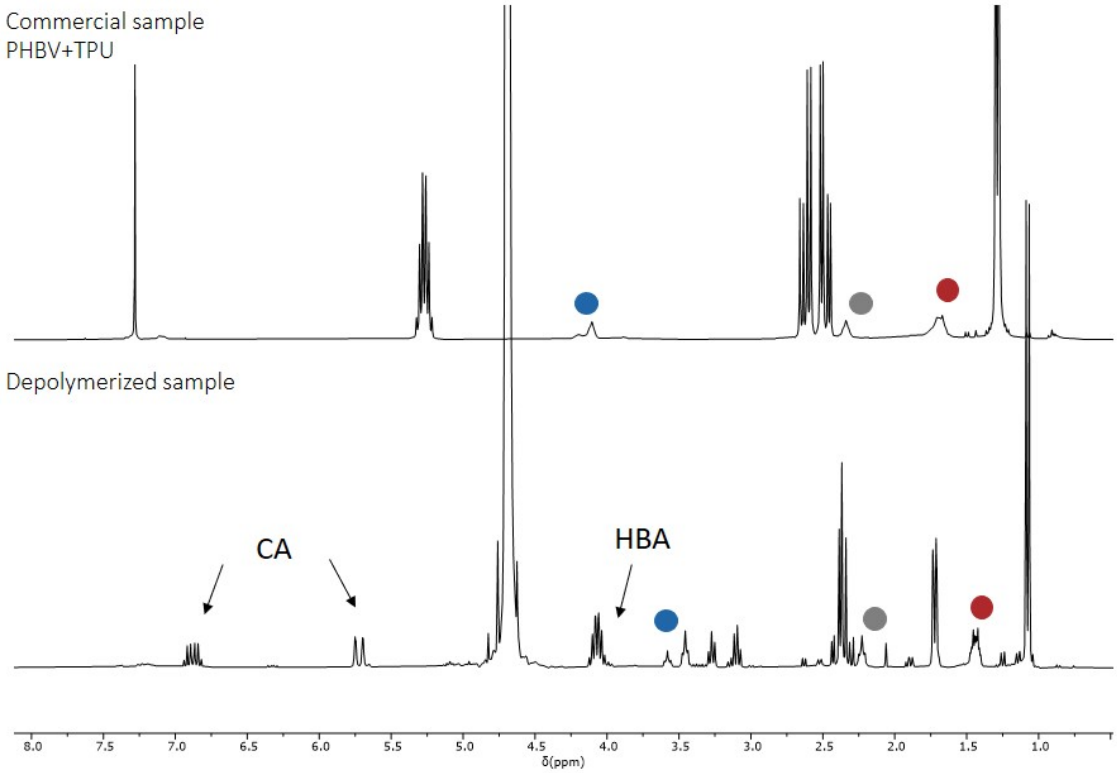

Figure S15. ^{1}H NMR comparison of commercial sample PHBV+TPU with the depolymerized sample. The colored circles indicate the presence of TPU before and after the depolymerization.

Computational results

Computational results were obtained using the M06-2X DFT method, as implemented in the Gaussian 09 package, version D.01.[3] Selection of Minessota functional was dictated by its high performance for main group thermochemistry, kinetics, and non-covalent interactions,[4] as well as by our own long experience in applying this functional in studying diverse bio-organic reactions with many successful outcomes.[5–10] Moreover, the chosen M06-2X functional was demonstrated to provide close to experimental energetics, also in the case of systems involving the participation of taurine, used to study the ring-opening polymerization (ROP) of cyclic monomers.[11] The 6-31+G(d,p) basis set, with polarization functions on s and p orbitals together with diffuse functions added to p orbitals was employed. To mimic the influence of the water environment, the conductor-like polarizable continuum model (CPCM) was used with a dielectric constant (ε) set to 78.[12–14] Hessian matrices were computed at the same levels of theory, confirming that the localized structures correspond to minima or transition states, TSs (zero or one negative eigenvalue of the diagonalized Hessians, respectively). Subsequently, zero-point vibrational energies (ZPEs) were added to the electronic energies to account for the nuclear vibrational contributions. The IRC paths were traced down on the potential energy surface to verify that the obtained TSs are related to the desired minima.

Two distinguished groups of models were prepared to investigate the various possible mechanisms of elimination reactions. In the first group, taurine is assumed to be inactive, while in the second group, elimination is governed by the active participation of taurine in the chemical transformations. Both groups were further subdivided based on the strong dependence of substrate and taurine protonation states on the pH conditions of the experiment. The first group was divided into three subgroups representing basic, neutral, and acidic conditions, while the second into four with basic (pH > 8), moderate (7 < pH < 8), acidic (4 < pH < 7), and highly acidic (pH < 1) conditions. The pKa values for the titratable groups of 3-hydroxybutyric acid monomer and taurine were predicted using Graph Neural Network using Graph-pKa software[15], and are presented in Figure S1, with the assigned protonation states for the corresponding pH conditions shown in Table S1.

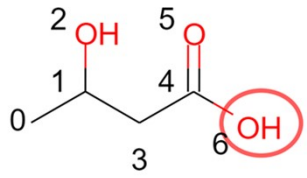

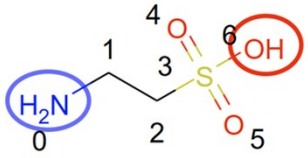

Most acidic pK_a: 4.61	
95% CI: [4.19-5.03]	
Atom index	Micro pK_a (acidic)
6	4.61
2	14.18

Most basic pK_a: None	
95% CI: None	
Atom index	Micro pK_a (basic)

Most acidic pK_a: 1.24	
95% CI: [0.69-1.79]	
Atom index	Micro pK_a (acidic)
6	1.24
0	19.28

Most basic pK_a: 8.87	
95% CI: [7.98-9.76]	
Atom index	Micro pK_a (basic)
0	8.87

Figure S16. Predicted pKa values for the carboxyl group of the hydroxy acid and amino and sulfonyl taurine groups using the Graph Neural Networks.

Table S2. Assumed protonation states of the substrate and taurine in prepared reaction models together with energy potential barriers with zero point corrections computed for the rate-determining steps (rds).

pH conditions	Protonation state		Energy barrier of rds (kcal·mol^{-1})	
	hydroxy acid	taurine	w/o taurine	w taurine
Basic	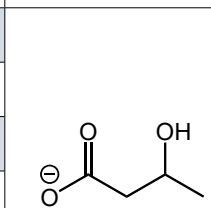	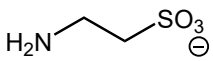	27.3	38.3
pH > 8.4				
Moderate acidic		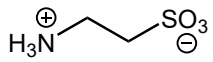	42.3	34.1
4.41 < pH < 8.4				
pH = 5.5				
Acidic				
pH < 4.41	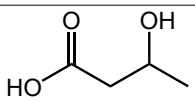		22.8	44.0
Highly acidic				
pH < 1		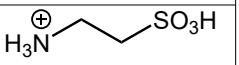		32.8[(1)] / 43.3[(2)]

(1) Concerted mechanism. See Scheme S7; (2) stepwise mechanism. See Scheme S8.

Computational results for elimination reaction without involvement of taurine.

Basic conditions (pH > 7)	Moderate conditions (pH ≈ 7)	Acidic conditions (pH < 7)
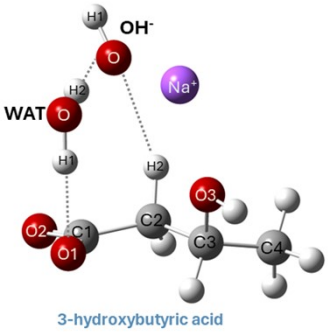	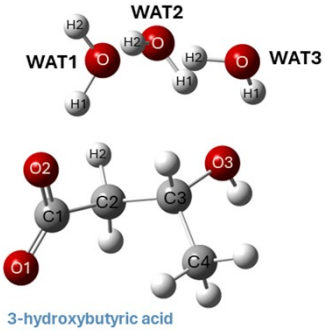	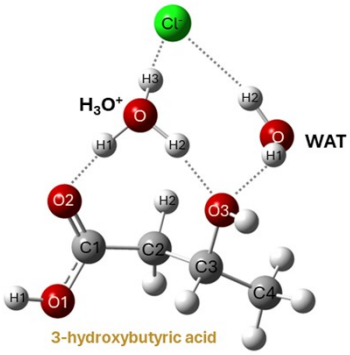

Figure S17. Structures of three molecular models used as a starting point for the computational study of the elimination of 3-hydroxybutyric acid monomer to the crotonic acid without the involvement of a taurine molecule.

Table S3. Key distances for stationary structures optimized and characterized at M06-2X/6-31+G(d,p)/CPCM=water level of theory along the elimination reaction of 3-hydroxybutyric acid monomer to the crotonic acid at basic conditions without the participation of taurine. Values are provided in Å.

Distance	RC	TS1	INT1	TS2	PC
d(C1-C2)	1.54	1.47	1.45/1.45	1.47	1.51
d(C2-C3)	1.52	1.50	1.49/1.49	1.39	1.34
d(C3-C4)	1.52	1.53	1.53/1.53	1.51	1.50
d(C1-O1)	1.26	1.30	1.30/1.31	1.30	1.27
d(C1-O2)	1.26	1.27	1.28/1.28	1.28	1.25
d(O1-H1^{wat})	1.97	1.64	1.48/1.47	1.51	1.58
d(C2-H2)	1.10	1.54	1.73/1.73	2.14	3.72
d(H2-O^{OH-})	2.44	1.14	1.05/1.05	0.98	1.08
d(C3-O3)	1.44	1.48	1.48/1.48	1.96	3.53
Imaginary wavenumber (cm^{-1})		608.29*i*		382.95*i*	

Table S4. Key distances for stationary structures optimized and characterized at M06-2X/6-31+G(d,p)/CPCM=water level of theory along the elimination reaction of 3-hydroxybutyric acid monomer to the crotonic acid explored at **moderate conditions** without participation of taurine. Values are provided in Å.

Distance	RC	INT1	TS1	INT2	TS2	INT3	PC
d(C1-C2)	1.53	1.51	1.45	1.40/1.40	1.44	1.48	1.50
d(C2-C3)	1.53	1.52	1.51	1.49/1.49	1.38	1.34	1.33
d(C3-C4)	1.52	1.52	1.52	1.52/1.52	1.50	1.49	1.50
d(C1-O1)	1.28	1.35	1.37	1.40/1.39	1.37	1.35	1.26
d(C1-O2)	1.25	1.20	1.23	1.25/1.25	1.23	1.21	1.27
d(O1-H1^{wat1})	1.54	0.97	0.97	0.97/0.97	0.97	0.97	1.63
d(O^{wat1}-H1^{wat1})	1.02	3.85	3.49	3.42/3.42	3.68	4.85	1.00
d(C2-H2)	1.10	1.10	1.39	1.96/1.96	2.34	2.68	3.44
d(O^{wat1}-H2)	2.86	2.46	1.25	1.00/1.00	0.97	0.96	0.97
d(C3-O3)	1.44	1.43	1.45	1.48/1.47	2.04	3.46	5.68
d(H1^{wat1}-O3)	3.65	4.67	4.69	4.72/4.72	4.86	6.35	0.97
Imaginary wavenumber (cm^{-1})			1239.85*i*		367.97*i*		

Table S5. Key distances for stationary structures optimized and characterized at M06-2X/6-31+G(d,p)/CPCM=water level of theory along the elimination reaction of 3-hydroxybutyric acid monomer to the crotonic acid explored at **acidic conditions** without participation of taurine. Values are provided in Å.

Distance	RC	TS1	INT1	TS2	**PC**

d(C1-C2)	1.51	1.40	1.35/1.35	1.38	1.47
d(C2-C3)	1.54	1.52	1.49/1.49	1.41	1.34
d(C3-C4)	1.52	1.52	1.52/1.52	1.50	1.49
d(C1-O1)	1.23	1.30	1.34/1.33	1.30	1.23
d(C1-O2)	1.32	1.32	1.35/1.35	1.33	1.33
d(O1-H1^{H3O+})	1.49	1.05	1.01/1.01	1.04	1.64
d(O^{H3O+}-H1^{H3O+})	1.03	1.43	1.58/1.58	1.46	1.00
d(C2-H2)	1.09	1.50	3.04/2.95	3.06	3.36
d(H2-O^{wat})	2.69	1.15	0.97/0.98	0.97	0.98
d(C3-O3)	1.44	1.45	1.48/1.48	1.83	3.11
d(H1^{wat}-O3)	2.13	2.12	1.38/1.38	1.04	1.00
d(H1^{wat}-O^{wat})	0.97	0.98	1.07/1.07	1.48	1.63
Imaginary wavenumber (cm^{-1})		719.00*i*		362.99*i*	

Table S6. Relative energies computed at M06-2X/6-31+G(d,p)/CPCM=water level of theory for stationary points optimized and characterized along the elimination reaction of 3-hydroxybutyric acid monomer to the crotonic acid at basic and acidic conditions without participation of taurine.

Basic conditions						
	E[Hartree]	ΔE(kcal/mol)	ZPE(kcal/mol)	ΔZPE(kcal/mol)	ΔE+ΔZPE (kcal/mol)	ΔE+ΔE$_{Therm}$ (kcal/mol)
RC	-696.89	0.0	93.85	0.00	0.0	0.0
TS1	-696.86	20.4	90.80	-3.05	17.3	16.8
INT 1	-696.87	18.0	92.15	-1.70	16.3	16.2
INT 1	-696.87	18.0	92.15	-1.70	16.3	16.2
TS2	-696.85	29.2	91.27	-2.58	26.6	27.3
PC	-696.88	5.7	90.40	-3.46	2.3	3.8

Moderate conditions						
	E[Hartree]	ΔE(kcal/mol)	ZPE(kcal/mol)	ΔZPE(kcal/mol)	ΔE+ΔZPE (kcal/mol)	ΔE+ΔE$_{Therm}$ (kcal/mol)
RC	-611.59	0.0	117.77	0.00	0.0	0.0
INT 1	-611.55	24.0	116.84	-0.93	23.1	22.9
TS1	-611.54	34.7	113.93	-3.84	30.9	30.8
INT 2	-611.54	29.7	116.89	-0.88	28.8	29.4
INT 2	-611.54	29.7	116.89	-0.88	28.8	29.4
TS2	-611.52	44.6	114.54	-3.23	41.4	42.3

INT 3	-611.54	31.5	113.35	-4.42	27.1	29.2
PC	-611.58	4.5	115.37	-2.40	2.1	3.6

Acidic conditions						
	E[Hartree]	ΔE(kcal/mol)	ZPE(kcal/mol)	ΔZPE(kcal/mol)	ΔE+ΔZPE (kcal/mol)	$\Delta E+\Delta E_{Therm}$ (kcal/mol)
RC	-996.42	0.0	117.41	0.00	0.0	0.0
TS1	-996.38	22.7	115.12	-2.29	20.5	19.3
INT 1	-996.39	19.2	116.88	-0.53	18.7	18.5
INT 1	-996.39	19.3	116.66	-0.75	18.5	18.4
TS2	-996.38	24.4	116.10	-1.31	23.1	22.8
PC	-996.41	1.6	115.16	-2.25	-0.7	0.3

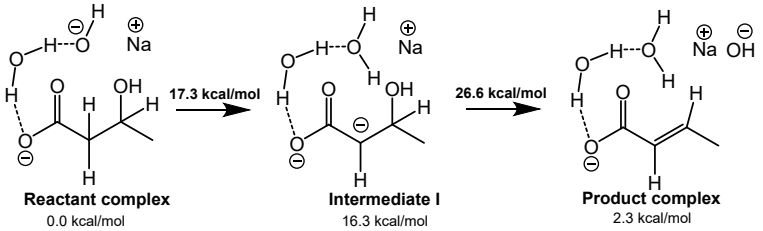

Scheme S1. Reaction mechanism at basic conditions.

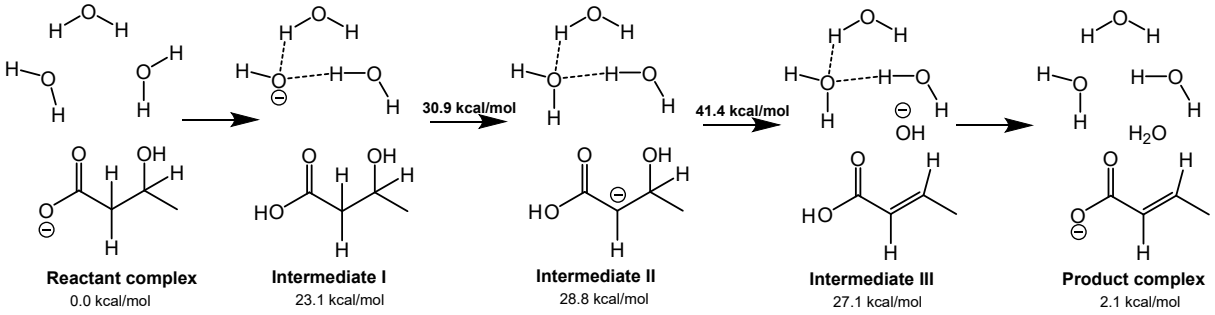

Scheme S2. Reaction mechanism at moderate conditions.

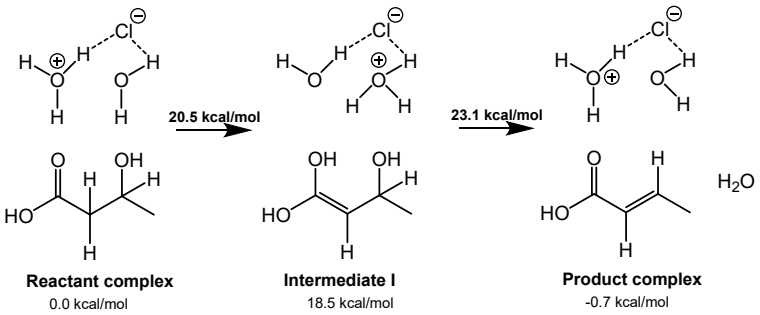

Scheme S3. Reaction mechanism at acidic conditions.

Computational results for elimination reaction with active participation of taurine.

Basic conditions pH > 8.4	Moderate conditions 4.4 < pH < 8.4	Acidic conditions pH < 4.4
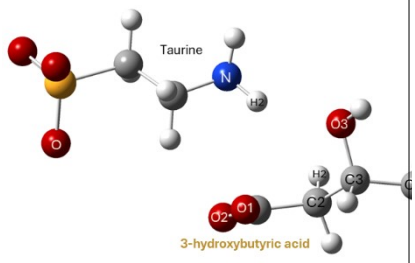	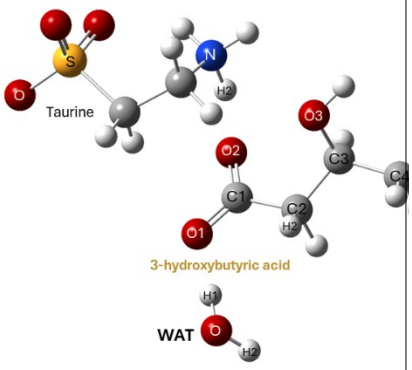	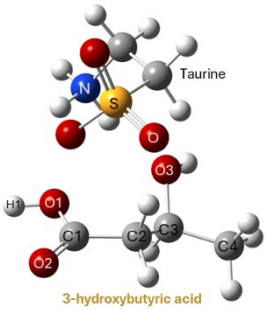

Figure S18. The structures of the molecular models used as a starting point for the computational study of the elimination of 3-hydroxybutyric acid monomer to the crotonic acid with the active participation of taurine molecule at acidic, moderate, and basic conditions.

Table S7. Key distances for stationary structures optimized and characterized at M06-2X/6-31+G(d,p)/CPCM=water level of theory along the elimination reaction of 3-hydroxybutyric acid monomer to the crotonic acid at basic conditions.

Distance	RC	TS1	INT1	TS2	PC
d(C1-C2)	1.54	1.45	1.39/1.39	1.45	1.51
d(C2-C3)	1.52	1.50	1.48/1.48	1.38	1.34
d(C3-C4)	1.52	1.53	1.53/1.53	1.51	1.50
d(C1-O1)	1.26	1.28	1.39/1.39	1.34	1.26
d(C1-O2)	1.26	1.31	1.27/1.27	1.24	1.26
d(C2-H2)	1.08	1.88	3.26/3.24	3.23	3.87
d(H2-N^{Tau})	3.61	1.08	1.02/1.02	1.05	1.76
d(C3-O3)	1.43	1.47	1.47/1.47	2.05	3.33
d(O3-H2)	2.55	2.27	2.04/2.02	1.70	1.00
d(O1-$H1^{Tau}$)	3.28	1.70	1.00/1.00	1.04	1.98
d(N^{Tau}-$H1^{Tau}$)	1.01	1.02	1.78/1.77	1.56	1.03
Imaginary wavenumber (cm^{-1})		227.49*i*		377.37*i*	

Table S8. Key distances for stationary structures optimized and characterized at M06-2X/6-31+G(d,p)/CPCM=water level of theory along the elimination reaction of 3-hydroxybutyric acid monomer to the crotonic acid at **moderate conditions.**

Distance	RC	TS1	INT1	TS2	INT2	TS3	PC
d(C1-C2)	1.53	1.46	1.37/1.37	1.42	1.48/1.49	1.49	1.50
d(C2-C3)	1.52	1.50	1.49/1.49	1.41	1.34/1.34	1.34	1.33
d(C3-C4)	1.52	1.52	1.52/1.52	1.51	1.49/1.49	1.50	1.50
d(C1-O1)	1.26	1.34	1.37/1.37	1.36	1.33/1.32	1.31	1.29
d(C1-O2)	1.27	1.25	1.29/1.29	1.25	1.22/1.22	1.23	1.24
d(C2-H2)	1.10	1.39	3.64/3.6	3.68	3.95/4.12	4.08	3.95
d(H2-O^{Wat})	3.42	1.25	0.96/0.96	0.97	0.96/0.97	0.97	0.98
d(C3-O3)	1.43	1.45	1.46/1.46	1.79	3.39/4.17	4.27	4.47
d(O3-$H1^{Tau}$)	2.49	2.12	1.89/1.95	1.15	1.00/0.96	0.96	0.96
d(N^{Tau}-$H1^{Tau}$)	1.02	1.02	1.03/1.03	1.35	1.76/3.54	3.56	3.47
d($H1^{Wat}$-O^{Wat})	0.99	1.59	1.83/1.83	1.80	1.69/3.06	3.06	3.11
d($H1^{Wat}$-O1)	1.71	1.02	0.98/0.98	0.98	0.99/1.08	1.19	1.48
d($H1^{Wat}$-N^{Tau})	5.51	5.23	4.73/4.90	4.84	4.72/1.46	1.29	1.10
Imaginary wavenumber (cm^{-1})		1436.86*i*		644.24*i*		620.44*i*	

Table S9. Key distances for stationary structures optimized and characterized at M06-2X/6-31+G(d,p)/CPCM=water level of theory along the elimination reaction of 3-hydroxybutyric acid monomer to the crotonic acid at **acidic conditions.**

Distance	RC	TS1	PC
d(C1-C2)	1.51	1.43	1.47
d(C2-C3)	1.53	1.42	1.34
d(C3-C4)	1.52	1.50	1.49
d(C1-O1)	1.34	1.37	1.21
d(C1-O2)	1.21	1.23	1.35
d(H1-O1)	0.97	0.97	0.97
d(C2-H2)	1.10	1.81	3.28
d(H2-O^{Tau})	2.72	1.02	2.00
d(H2-O3)	2.53	2.60	0.97
d(C3-O3)	1.43	1.80	3.83
d(O3-$H1^{Tau}$)	1.83	1.08	1.72
d(N^{Tau}-$H1^{Tau}$)	10.4	1.49	1.05
Imaginary wavenumber (cm^{-1})		424.51*i*	

Table S10. Relative energies computed at M06-2X/6-31+G(d,p)/CPCM=water level of theory for stationary points optimized and characterized along the elimination reaction of 3-hydroxybutyric acid monomer to the crotonic acid **at basic, moderate, and acidic conditions** with active participation of taurine for Model A and B.

Basic conditions						
	E[Hartree]	ΔE(kcal/mol)	ZPE(kcal/mol)	ΔZPE(kcal/mol)	ΔE+ΔZPE (kcal/mol)	$\Delta E+\Delta E_{Therm}$ (kcal/mol
RC	-1140.73	0.0	132.06	0.00	0.0	0.0
TS1	-1140.67	40.8	130.84	-1.23	39.6	38.3
INT 1	-1140.70	22.8	132.15	0.08	22.9	22.4
INT 1	-1140.70	22.9	132.06	0.00	22.9	22.4
TS2	-1140.67	37.5	129.36	-2.70	34.8	34.2
PC	-1140.73	3.4	129.80	-2.26	1.2	2.4

Moderate conditions						
	E[Hartree]	ΔE(kcal/mol)	ZPE(kcal/mol)	ΔZPE(kcal/mol)	ΔE+ΔZPE (kcal/mol)	$\Delta E+\Delta E_{Therm}$ (kcal/mol
RC	-1217.63	0.0	156.69	0.00	0.0	0.0
TS1	-1217.57	38.3	153.70	-2.99	35.3	34.1
INT 1	-1217.59	24.4	155.52	-1.17	23.2	23.4
INT 1	-1217.59	23.8	155.13	-1.56	22.2	22.5
TS2	-1217.57	35.9	153.26	-3.43	32.5	32.6
INT 2	-1217.61	13.5	153.71	-2.98	10.5	12.5
INT 2	-1217.62	7.6	153.15	-3.55	4.1	5.9
TS3	-1217.62	7.8	151.60	-5.09	2.7	4.2
PC	-1217.62	7.0	154.01	-2.69	4.3	5.9

Acidic conditions						
	E[Hartree	ΔE(kcal/mol)	ZPE(kcal/mol)	ΔZPE(kcal/mol)	ΔE+ΔZPE	$\Delta E+\Delta E_{Therm}$

	]				(kcal/mol)	(kcal/mol
RC	-1141.67	0.0	150.39	0.00	0.0	0.0
TS1	-1141.59	48.7	145.94	-4.45	44.2	44.0
PC	-1141.65	10.1	147.52	-2.87	7.3	9.2

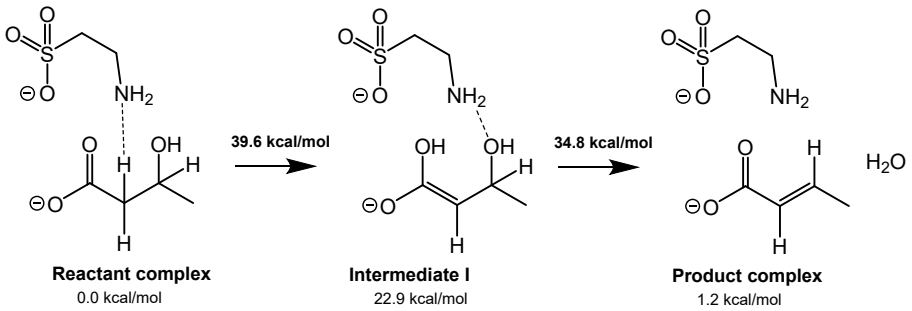

Scheme S4. Reaction mechanism at basic conditions.

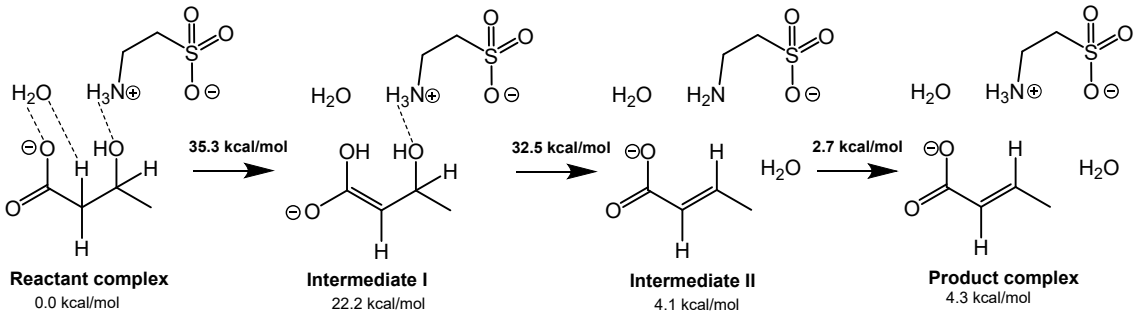

Scheme S5. Reaction mechanism at moderate conditions.

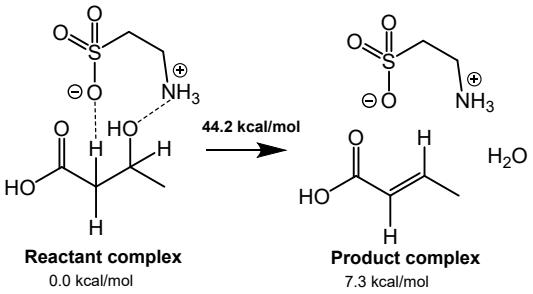

Scheme S6. Reaction mechanism at acidic conditions.

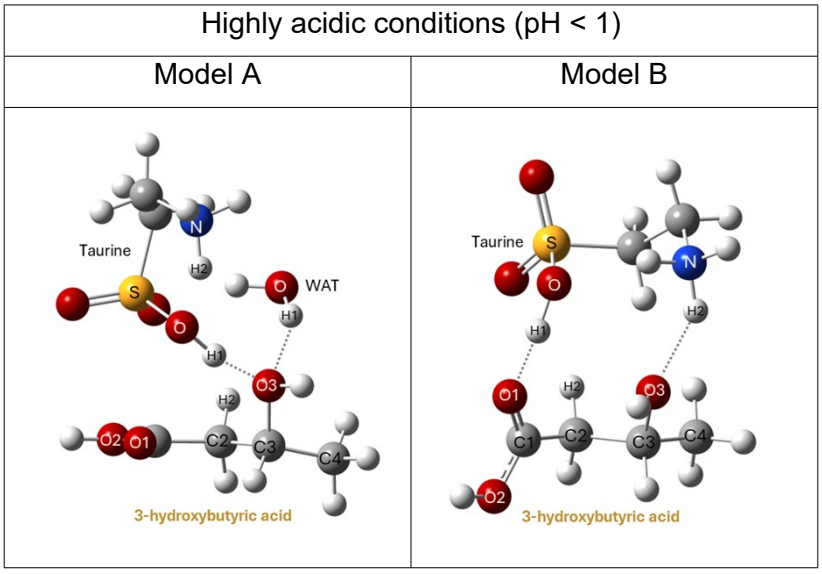

Figure S19. Structures of two molecular models used as a starting point for the computational study of the elimination of 3-hydroxybutyric acid monomer to the crotonic acid with active participation of taurine molecule in highly acidic conditions.

Table S11. Key distances for stationary structures optimized and characterized at M06-2X/6-31+G(d,p)/CPCM=water level of theory along the elimination reaction of 3-hydroxybutyric acid monomer to the crotonic acid at highly acidic conditions with the active participation of taurine, Model A. Values are provided in Å.

Distance	RC	TS1	PC
d(C1-C2)	1.50	1.46	1.48
d(C2-C3)	1.52	1.42	1.34
d(C3-C4)	1.52	1.50	1.49
d(C1-O1)	1.21	1.22	1.22
d(C1-O2)	1.33	1.35	1.34
d(C2-H2)	1.10	1.50	2.55
d(H2-O^{WAT})	2.69	1.14	0.97
d(C3-O3)	1.45	1.84	3.38
d(O3-$H1^{Tau}$)	1.49	1.00	1.06
d(O^{Tau}-$H1^{Tau}$)	1.04	1.59	1.39
Imaginary wavenumber (cm^{-1})		728.33*i*	

Table S12. Key distances for stationary structures optimized and characterized at M06-2X/6-31+G(d,p)/CPCM=water level of theory along the elimination reaction of 3-hydroxybutyric acid monomer to the crotonic acid at **highly acidic conditions** with the active participation of taurine, **Model B**. Values are provided in Å.

Distance	RC	TS1	INT1	TS2	INT2	TS3	PC
d(C1-C2)	1.50	1.48	1.49/1.49	1.39	1.36/1.34	1.39	1.48
d(C2-C3)	1.54	1.54	1.53/1.53	1.52	1.51/1.50	1.41	1.34
d(C3-C4)	1.52	1.52	1.51/1.51	1.52	1.52/1.52	1.49	1.49
d(C1-O1)	1.23	1.27	1.26/1.26	1.31	1.33/1.35	1.30	1.22
d(C1-O2)	1.32	1.28	1.28/1.29	1.32	1.33/1.35	1.32	1.33
d(O1-$H1^{Tau}$)	1.47	1.00	1.06/1.05	0.99	0.98/0.97	1.07	1.78
d(O^{Tau}-$H1^{Tau}$)	1.04	2.16	2.96/2.96	2.99	3.01/3.72	4.51	3.87
d(C2-H2)	1.09	1.10	1.10/1.10	1.49	1.79/5.13	4.08	3.98
d(H2-O^{Tau})	3.28	2.87	2.17/2.17	1.16	1.03/0.97	0.97	0.97
d(C3-O3)	1.43	1.44	1.45/1.45	1.45	1.45/1.45	1.42	3.44
d($H1^{Tau}$-O3)	2.71	1.77	1.44/1.44	1.75	1.82/1.91	1.07	0.98
Imaginary wavenumber (cm^{-1})		172.14*i*		883.27*i*		551.02*i*	

Table S13. Relative energies computed at M06-2X/6-31+G(d,p)/CPCM=water level of theory for stationary points optimized and characterized along the elimination reaction of 3-hydroxybutyric acid monomer to the crotonic acid at highly acidic conditions with active participation of taurine for Model A and B.

Model A						
	E[Hartree]	ΔE(kcal/mol)	ZPE(kcal/mol)	ΔZPE(kcal/mol)	ΔE+ΔZPE (kcal/mol)	$\Delta E+\Delta E_{Therm}$ (kcal/mol
RC	-1218.51	0.0	173.59	0.00	0.0	0.0
TS1	-1218.45	37.4	169.60	-3.99	33.4	32.8
PC	-1218.50	6.6	170.59	-3.00	3.6	4.3

Model B					
	E[Hartree]	ΔE(kcal/mol)	ZPE(kcal/mol)	ΔZPE(kcal/mol)	ΔE+ΔZPE (kcal/mol)
RC	-1142.10	0.0	157.98	0.00	0.00
TS1	-1142.08	12.6	158.43	0.46	13.10
INT1	-1142.08	10.3	158.20	0.23	10.54
INT1	-1142.08	10.3	158.21	0.23	10.55
TS2	-1142.05	27.5	155.37	-2.60	24.94
INT2	-1142.05	26.7	157.35	-0.62	26.08
INT2	-1142.05	27.2	157.78	-0.20	26.95
TS3	-1142.02	47.1	154.17	-3.80	43.27
PC	-1142.08	12.0	155.06	-2.91	9.12

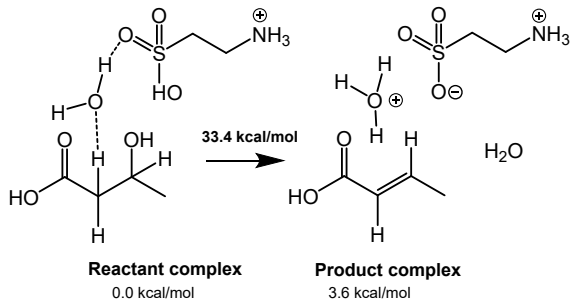

Scheme S7. Concerted reaction mechanism at highly acidic conditions.

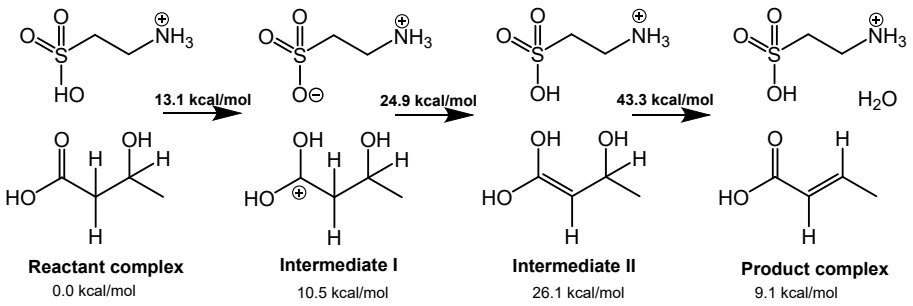

Scheme S8. Step-wise reaction mechanism at highly acidic conditions.

Table S14. Relative energies computed at M06-2X/6-31+G(d,p)/CPCM=water level of theory for stationary points optimized and characterized along the depolymerization reaction catalyzed by taurine.

Basic conditions						
	E[Hartree]	ΔE(kcal/mol)	ZPE(kcal/mol)	ΔZPE(kcal/mol)	ΔE+ΔZPE (kcal/mol)	$\Delta E+\Delta E_{Therm}$ (kcal/mol)
RC	-1524.02	0.0	220.56	0.00	0.0	0.0
TS1	-1523.99	23.3	218.09	-2.47	20.8	18.7
INT 1	-1523.99	18.9	220.49	-0.07	18.8	17.1
INT 1	-1524.00	15.7	220.60	0.04	15.7	13.7
TS2	-1523.99	18.9	218.45	-2.11	16.8	14.5
PC	-1524.02	-1.1	221.35	0.79	-0.3	-1.1

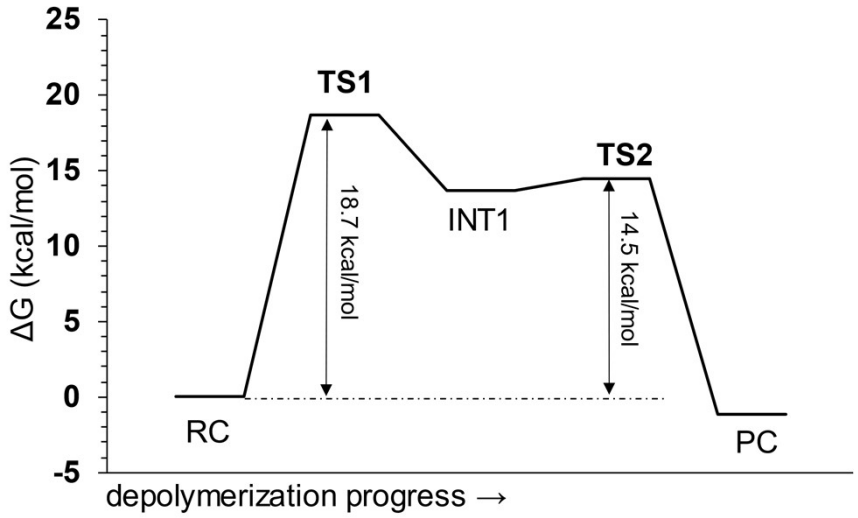

Figure S17. Free energy profile for the depolymerization reaction catalyzed by taurine with thermal corrections.

Table S15. Key distances (in Å) of optimized and characterized stationary points along the depolymerization process catalyzed by taurine at M06-2X level with the continuum water model (CPCM).

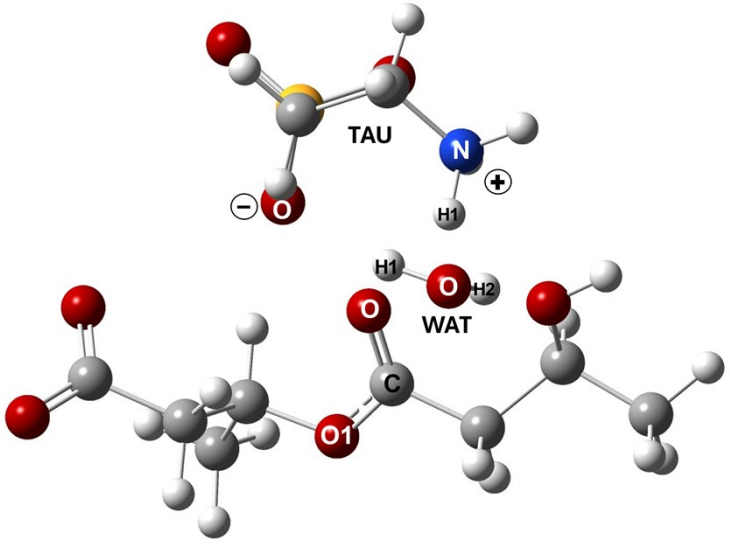

Distance	RC	TS1	INT1	TS2	PC
C^{poly}-O^{WAT}	2.79	1.69	1.46/1.39	1.35	1.32
O^{WAT}-$H1^{WAT}$	0.98	1.08	1.50/2.54	2.50	3.59
$H1^{WAT}$-O^{TAU}	1.82	1.36	1.03/1.04	1.50	1.85
C^{poly}-O^{poly}	1.22	1.31	1.37/1.37	1.30	1.22
C^{poly}-$O1^{poly}$	1.33	1.34	1.38/1.45	1.73	2.85
O^{poly}-$H1^{TAU}$	1.86	1.09	1.02/1.01	1.14	1.79
N^{TAU}-$H1^{TAU}$	1.04	1.45	1.66/1.70	1.37	1.04
$O1^{poly}$-$H1^{WAT}$	3.19	2.89	3.12/1.47	1.03	0.98
Imaginary wavenumber (cm^{-1})		-313.26*i*		-375.93*i*	

References

(1) Cheong, S.; Clomburg, J. M.; Gonzalez, R. Energy- and Carbon-Efficient Synthesis of Functionalized Small Molecules in Bacteria Using Non-Decarboxylative Claisen Condensation Reactions. *Nat. Biotechnol. 2016 345* 2016, *34* (5), 556–561. https://doi.org/10.1038/nbt.3505.

(2) Orrego, A. H.; Rubanu, M. G.; López, I. L.; Andrés-Sanz, D.; García-Marquina, G.; Pieslinger, G. E.; Salassa, L.; López-Gallego, F. ATP-Independent and Cell-Free Biosynthesis of β-Hydroxy Acids Using Vinyl Esters as Smart Substrates. *Angew. Chemie Int. Ed.* 2023, *62* (13), e202218312. https://doi.org/10.1002/ANIE.202218312.

(3) Frisch, M.J.; Trucks, G.W.; Schlegel, H.B.; Scuseria, G.E.; Robb, M.A.; Cheeseman, J.R.; Scalmani, G.; Barone, V.; Mennucci, B.; Petersson, G.A.; Nakatsuji, H.; Caricato, M.; Li, X.; Hratchian, H.P.; Izmaylov, A.F.; Bloino, J.; Zheng, G.; Sonnenberg, J.L., D. J. *No Title*, Gaussian 0.; Gaussian Inc, Ed.; Wallingford, 2010.

(4) Mardirossian, N.; Head-Gordon, M. Thirty Years of Density Functional Theory in Computational Chemistry: An Overview and Extensive Assessment of 200 Density Functionals. *Mol. Phys.* 2017, *115* (19), 2315–2372. https://doi.org/10.1080/00268976.2017.1333644.

(5) Ferrer, S.; Moliner, V.; Świderek, K. Electrostatic Preorganization in Three Distinct Heterogeneous Proteasome β-Subunits. *ACS Catal.* 2024, *14*, 15237–15249. https://doi.org/10.1021/ACSCATAL.4C04964.

(6) Świderek, K.; Velasco-Lozano, S.; Galmés, M.; Olazabal, I.; Sardon, H.; López-Gallego, F.; Moliner, V. Mechanistic Studies of a Lipase Unveil Effect of PH on Hydrolysis Products of Small PET Modules. *Nat. Commun.* 2023, *14* (1), 1–10. https://doi.org/10.1038/s41467-023-39201-1.

(7) Krzemińska, A.; Moliner, V.; Świderek, K. Dynamic and Electrostatic Effects on the Reaction Catalyzed by HIV-1 Protease. *J. Am. Chem. Soc.* 2016, *138* (50), 16283–16298. https://doi.org/10.1021/JACS.6B06856.

(8) Świderek, K.; Moliner, V. Revealing the Molecular Mechanisms of Proteolysis of SARS-CoV-2 Mpro by QM/MM Computational Methods. *Chem. Sci.* 2020, *11* (39), 10626–10630. https://doi.org/10.1039/D0SC02823A.

(9) Serrano-Aparicio, N.; Moliner, V.; Swiderek, K. Nature of Irreversible Inhibition of Human 20S Proteasome by Salinosporamide A. The Critical Role of Lys-Asp Dyad Revealed from Electrostatic Effects Analysis. *ACS Catal.* 2021, *11* (6), 3575–3589. https://doi.org/10.1021/ACSCATAL.0C05313.

(10) Galmés, M. i.; Nödling, A. R.; He, K.; Luk, L. Y. P.; Świderek, K.; Moliner, V. Computational Design of an Amidase by Combining the Best Electrostatic Features of Two Promiscuous Hydrolases. *Chem. Sci.* 2022, *13* (17), 4779–4787. https://doi.org/10.1039/D2SC00778A.

(11) Gabirondo, E.; Świderek, K.; Marin, E.; Maiz-Iginitz, A.; Larranaga, A.; Moliner, V.; Etxeberria, A.; Sardon, H. A Single Amino Acid Able to Promote High-Temperature Ring-Opening Polymerization by Dual Activation. *Adv. Sci.* 2024, *11* (16), 2308956. https://doi.org/10.1002/ADVS.202308956.

(12) Pascual-ahuir, J. L.; Silla, E.; Tuñon, I. GEPOL: An Improved Description of Molecular Surfaces. III. A New Algorithm for the Computation of a Solvent-Excluding Surface. *J. Comput. Chem.* 1994, *15* (10), 1127–1138. https://doi.org/10.1002/JCC.540151009.

(13) Miertuš, S.; Tomasi, J. Approximate Evaluations of the Electrostatic Free Energy and Internal Energy Changes in Solution Processes. *Chem. Phys.* 1982, *65* (2), 239–245. https://doi.org/10.1016/0301-0104(82)85072-6.

(14) Miertuš, S.; Scrocco, E.; Tomasi, J. Electrostatic Interaction of a Solute with a Continuum. A Direct Utilizaion of AB Initio Molecular Potentials for the Prevision of Solvent Effects. *Chem. Phys.* 1981, *55* (1), 117–129. https://doi.org/10.1016/0301-0104(81)85090-2.

(15) Xiong, J.; Li, Z.; Wan, G.; Fu, Z.; Zhong, F.; Xu, T.; Liu, X.; Huang, Z.; Liu, X.; Chen, K.; Jiang, H.; Zheng, M. Multi-Instance Learning of Graph Neural Networks for Aqueous PKa Prediction.

Bioinformatics **2022**, *38* (3), 792–798. https://doi.org/10.1093/BIOINFORMATICS/BTAB714.